

A STUDY OF DOPPLER BEAM SWINGING USING AN IMAGING RADAR

B. L. Cheong^{1, 1}, T.-Y. Yu², R. D. Palmer¹, G.-F. Yang³, M. W. Hoffman⁴, S. J. Frasier⁵ and F. J. López-Dekker⁵

¹ School of Meteorology, University of Oklahoma, Norman, USA

² School of Electrical and Computer Engineering, University of Oklahoma, Norman, USA

³ Institution of Space Science, National Central University, Taiwan

⁴ Department of Electrical Engineering, University of Nebraska, Lincoln, USA

⁵ Department of Electrical and Computer Engineering, University of Massachusetts, Amherst, USA

1. INTRODUCTION

In this paper, a study of the Doppler Beam Swinging (DBS) technique for horizontal wind estimation using an imaging radar is presented. The primary goal is to quantify effects of temporal and spatial inhomogeneities in the quality of DBS wind estimates. The DBS technique has been extensively applied to Mesosphere-Stratosphere-Troposphere (MST) radars, including boundary layer radars (BLR), to obtain a profile of wind vectors within the atmosphere (see Röttger and Larsen [1990] and references therein). The term DBS has been coined as MST radars that steer the beam in at least three directions to obtain a profile of the wind vector.

The data for this study were obtained using the Turbulent Eddy Profiler (TEP), which is a 915-MHz imaging BLR with an array of up to 64 receivers and has a 25° field of view [Mead et al., 1998; López-Dekker and Frasier, 2004; Cheong et al., 2004]. Using adaptive array processing, 3-D volumetric images can be constructed within the field of view with a temporal resolution of approximately 2.5 s. For this study, images of signal-to-noise ratio (SNR) and radial velocity will be emphasized. Radial velocity estimates from the regions with sufficiently high SNR (typically > 3 dB) are extracted for horizontal wind extraction through DBS. For each scan, a significantly over-determined DBS equation set (is used to compute the horizontal velocity and that estimate serves as the reference for comparison. Conventional DBS measurements are produced from the same data using a vertical beam and two off-vertical beams at a zenith angle of 10°. As might be expected, these *under-sampled* DBS wind estimates will show effects of both reflectivity and radial velocity inhomogeneities.

2. THE TURBULENT EDDY PROFILER

The TEP radar consists of a horn antenna for transmission and an array of up to 64 microstrip patch elements separated by approximately 0.57 m, which are used for reception [Mead et al., 1998; López-Dekker and Frasier, 2004]. Signals from each receiver are sent through a low-noise amplifier before being fed into the data acquisition system. The in-phase and quadrature signals are digitized and stored on disk for offline processing. By coherently combining the signals from the individual elements, it is possible to image the atmosphere in a conical shaped volume above the radar. A depiction of the TEP imaging concept is provided in Figure 1. The transmit beamwidth of TEP is relatively wide, which defines the field of view of the radar. Using beamforming, which is fundamentally a procedure of combining signals from all receivers in order to synthesize narrow focused beams within the transmit beam, it is possible to create an image of the atmosphere above the radar. This process is conducted for each range gate individually, resulting in a 3-D image.

3. GENERAL ATMOSPHERIC STRUCTURE DURING EXPERIMENT

After successful phase calibration, images of SNR and radial velocity are obtained through a pulse-pair beamforming (PPB) process [Cheong et al., 2004]. Radial velocity measurements that couple with sufficiently good SNR are selectively fed into the DBS processing. In the present study, Capon-based adaptive beamforming is used and the beam is steered in a 1°-increment within the field of view, resulting in each image with approximately 500 pixels, or beam positions. Of course, the effective angular resolution for the TEP radar using Fourier beamforming is approximately 3.5°. Using the adaptive Capon beamforming, however, we expect an improved resolution of 1.5°. The data shown in Figure 2 represent a 20-minute time

¹ Corresponding author address: Boon Leng Cheong, University of Oklahoma, School of Meteorology, 100 East Boyd Street, Suite 1310, Norman, OK 73019; e-mail: boonleng@ou.edu

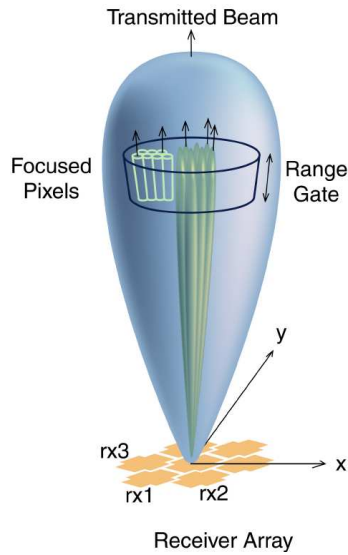


Figure 1: An artist's depiction of the TEP radar and general imaging process. The transmit beam is shown as the relatively wide angular region. Using digital beamforming, small-scale structures within the field of view can be extracted.

history of vertical-beam SNR and radial velocity. This figure shows the data with the full resolution of the TEP radar, i.e., 2.5 s in time and 33.3 m in range-gate spacing.

During the 20-minute data set, the convective boundary layer was well established, with the entrainment zone visible at an altitude of approximately 1 km.

4. OVERDETERMINED DOPPLER BEAM SWINGING

The traditional DBS technique is typically implemented using an algorithm based on Equation (1).

$$\begin{bmatrix} \sin \theta_1 \sin \phi_1 & \sin \theta_1 \cos \phi_1 & \cos \theta_1 \\ \sin \theta_2 \sin \phi_2 & \sin \theta_2 \cos \phi_2 & \cos \theta_2 \\ \vdots & \vdots & \vdots \\ \sin \theta_m \sin \phi_m & \sin \theta_m \cos \phi_m & \cos \theta_m \end{bmatrix} \begin{bmatrix} u \\ v \\ w \end{bmatrix} = \begin{bmatrix} v_r^{(1)} \\ v_r^{(2)} \\ \vdots \\ v_r^{(m)} \end{bmatrix} \quad (1)$$

Using the high-resolution TEP radar, however, a large number of beam positions is available for solving the DBS equations and this DBS-derived horizontal wind vector will serve as the reference for comparison, given that it represents the average wind field within the view of the radar. In particular, beam positions are used from an annulus of zenith angles of 4-11° for all azimuth angles. As a result, any azimuthal inhomogeneities are averaged and we maximize the number of beam positions for the over-determined DBS solution.

5. PRELIMINARY RESULTS

Using the TEP imaging radar, we are able to estimate maps of SNR and radial velocity for different temporal and spatial averaging. Figure 3 shows one such result for a 10-minute, 4-range-gate (133 m) average of the second half of the dataset at approximately 900 m. As expected, the SNR map (left panel) is relatively smooth, representing a homogeneous turbulence field. Further, the radial velocity field shows the expected linear variation in velocity from negative values (toward the radar) to positive values (away from radar). Assuming small vertical velocity, which is reasonable over a 10-minute average, the zero isodop is perpendicular to the wind direction. For a zenith angle of 10° and for only three beam positions (vertical and two

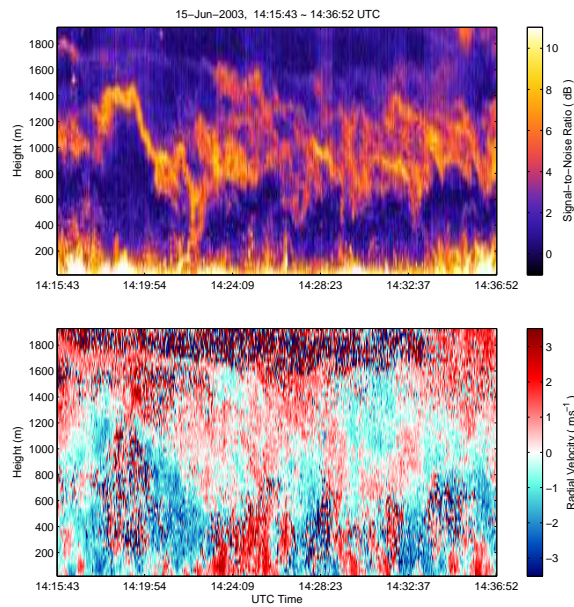


Figure 2: During the observation period, convective and mixing processes can be seen within the boundary layer. This provides strong signals for the imaging radar and the dataset is used for the preliminary study.

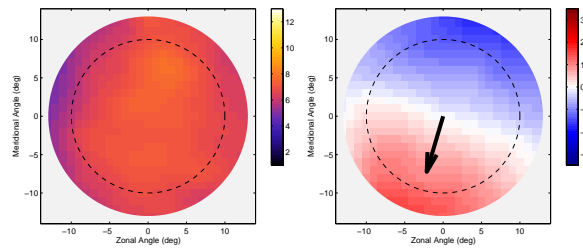


Figure 3: At approximately 900 m, 10-minute averaging of the second half of the dataset, smooth SNR (power) and radial velocity maps resulted from long-temporal averaging as one might expect.

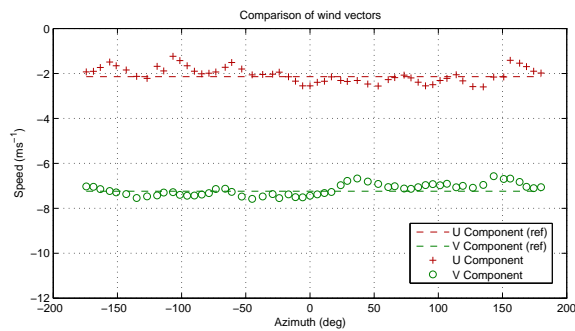


Figure 4: For a 10-minute averaging, DBS-derived u and v components are consistent with the reference for all azimuth angles.

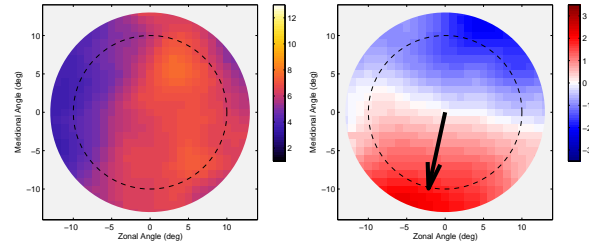


Figure 5: For this case, 30-second averaging is used resulting SNR and radial-velocity maps that are less uniform. One can see significant variations in both SNR and radial velocity maps.

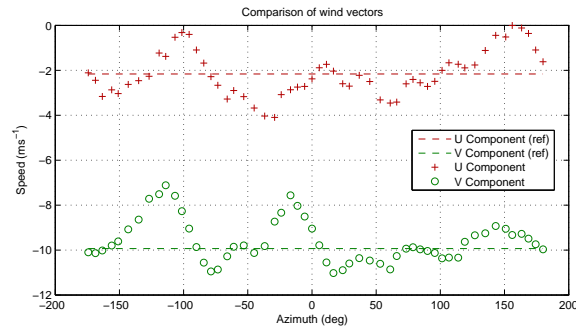


Figure 6: Wind vectors exhibit higher variations from the reference as the homogenous condition is no longer true, which can be seen more pronounced for azimuth = -90° to -150° .

off-vertical), the DBS method was implemented producing the results in Figure 4. The two off-vertical beams are separated in azimuth angle by 90° and this set of beams is rotated around all possible azimuth angles. By doing so, it is possible to study the effect of horizontal inhomogeneities in both the SNR and radial velocity fields. Given the 10-minute average, the results are quite good when compared to the reference velocity.

When the temporal averaging is reduced to only 30 sec, the results are significantly diminished. Figure 5 shows the SNR and radial velocity showing marked variability in both SNR and radial velocity. It is precisely this variability, or inhomogeneities, which is the reason for the poor comparison between the three-beam results and the reference velocities, which is shown in Figure 6. For example, azimuth angles of -90° to -150° show a significant decrease in SNR and corresponding erratic radial velocity behavior. As a result, the horizontal wind estimates using DBS are also corrupted. For this particular case, we can see that short-time averaged horizontal wind estimates would be problematic given the choice of azimuth angles.

6. FUTURE PLANS

Using the digital beamforming techniques, hundreds of beams can be formed simultaneously within the field of view. As a result, the horizontal distribution of SNR and radial velocity can be obtained at each range gate. This allows us to investigate the accuracy of DBS wind measurements for various configurations and atmospheric conditions. For example, the effect of temporal averaging, range-gate spatial average and radar sampling on DBS wind estimates in conjunction with the atmospheric homogeneities has been shown using the TEP. Comprehensive and quantitative comparisons of various DBS configurations such as 5 beam positions, different zenith angles, and the period of time-average are now planned. Moreover, the effect of inhomogeneities and horizontal shear on DBS will be investigated and quantified.

References

Cheong, B. L., M. W. Hoffman, R. D. Palmer, S. J. Frasier, and F. J. López-Dekker, 2004: Pulse pair beamforming and the effects of reflectivity field variations on imaging radars. *Radio Sci.*, **39**(RS3014), doi:10.1029/2002RS002843.

- López-Dekker, P., and S. J. Frasier, 2004: Radio acoustic sounding with a UHF volume imaging radar. *J. Atmos. Oceanic Technol.*, **21**, 766–776.
- Mead, J. B., G. Hopcraft, S. J. Frasier, B. D. Pollard, C. D. Cherry, D. H. Schaubert, and R. E. McIntosh, 1998: A volume-imaging radar wind profiler for atmospheric boundary layer turbulence studies. *J. Atmos. Oceanic Technol.*, **15**, 849–859.
- Röttger, J., and M. F. Larsen, 1990: *UHF/VHF radar techniques for atmospheric research and wind profiler applications*. p. 806. Am. Meteor. Soc., Boston, Mass.